Critical experiments and analyses at cryogenic temperature to promote a better understanding of mechanical properties in high-strength alloys

Osamu Umezawa and Kotobu Nagai

Citation: AIP Conference Proceedings **1574**, 327 (2014); doi: 10.1063/1.4860644
View online: http://dx.doi.org/10.1063/1.4860644
View Table of Contents: http://scitation.aip.org/content/aip/proceeding/aipcp/1574?ver=pdfcov
Published by the AIP Publishing

Critical Experiments and Analyses at Cryogenic Temperature to Promote a Better Understanding of Mechanical Properties in High-Strength Alloys

Osamu Umezawa[a] and Kotobu Nagai[b]

[a]Faculty of Engineering, Yokohama National University, 79-5 Tokiwadai, Hodogaya, Yokohama, 240-8501, Japan
[b]National Institute for Materials Science, 1-2-1 Sengen, Tsukuba, 305-0047, Japan

Abstract. Mechanical test at cryogenic temperature shows the advantages on characterization of deformation and cracking behavior in alloys from the viewpoint of microstructure. Microstructural crack initiation in high-cycle fatigue is clearly detected at the specimen interior. The high-strength alloys also show higher strain rate dependence on tensile deformation and low temperature creep deformation under thermal activation process. Not only microstructural analyses using noble techniques but also modeling works on the subsurface crack generation and tensile deformation are focused.

Keywords: high-cycle fatigue, crack initiation, transgranular cracking, intergranular cracking, strain rate dependence, Taylor factor, critical resolved shear stress, thermal activation process, stress-strain curve
PACS: 62.20.mt

INTRODUCTION

As test temperature is lower below room temperature, the strength of an alloy increases.. This results from the decrease of thermal stress during dislocation motion. The critical resolved shear stress (CRSS) strongly depends on slip systems in the alloy. Heterogeneous deformation and localized yielding are normally enhanced, especially at low strains. As a result, the fracture toughness is lowered, and microstructural crack initiation in high-cycle fatigue has been clearly detected within the specimen interior. Transgranular cracking, intergranular cracking, non-metallic inclusions, or microstructural irregularities, may serve as the crack source, since strain incompatibility due to heterogeneous deformation at boundaries is highly developed [1-2]. Therefore, cryogenic fatigue tests in which the materials are immersed in liquid helium or nitrogen has advantages to enhance clear detection of microstructural cracking at lower cycles and with less environmental effects. High strength alloy also show higher strain rate dependence on tensile deformation at low temperatures and low- temperature creep deformation.

In this review, the advantage of cryogenic mechanical tests is discussed to promote better understanding of deformation and microstructural cracking in high-strength alloys. Taylor analysis under tension modes is adopted to discuss the heterogeneous deformation and subsurface crack initiation [3]. The description of stress-strain curves in tension is also described from both experimental and modeling works [4-7].

SUBSURFACE CRACK INITIATION IN HIGH-CYCLE FATIGUE

Cryogenic Fatigue Test

A number of studies have been conducted to clarify fatigue crack generation and growth mechanisms for high strength alloys. From the previous review in the reference [1], a change in crack initiation mechanism from specimen surface to specimen interior often introduces a plateau ("knee") followed by a rather sharp drop in the shape of S-N curve. As shown in Figure 1, the subsurface crack initiation can be detected in much wider stress ranges and at lower cycles. Even though the subsurface crack origins are related with various microstructural crackings or pre-existing defects, the subsurface initiation site is commonly formed as a Stage I crack in tension mode. The size is the most important parameter to determine if the crack becomes a fatal crack, and highly depends on the maximum cyclic stress range, which implies a ΔK_{th} threshold controlling mechanism. Kitagawa et al. [8] and

Advances in Cryogenic Engineering
AIP Conf. Proc. 1574, 327-332 (2014); doi: 10.1063/1.4860644

Murakami [9] proposed that the fatigue limit of the material containing pre-existing defects was determined from the relationship between the defect size and threshold stress range as illustrated in Figure 2(a). These ideas are based on the assumption that a small defect such as an inclusion is equivalent to a microcrack (Stage I crack) and that the microcrack growth is retained under the fatigue limit. In the range of 2a (crack length) > d* (threshold defect size), ΔK_{th} value determines the fatigue limit threshold stress range. When a Stage I crack becomes a critical size, only principal stress (Mode I) controls its propagation (Stage II). Then, an approximate equation simplified to give the maximum stress intensity range, ΔK_{Imax}, at the crack tip is roughly represented as follows:

$$\Delta K_{\mathrm{Im}ax} = A\Delta\sigma_{\max}\sqrt{\pi 2a} \tag{4}$$

where A is coefficient, $\Delta\sigma_{max}$ is maximum cyclic stress range and 2a is crack length.

According to the equation, the critical condition that a microcrack provides a fatal crack in a given stress range can be evaluated. Figure 2(b) represents the size of Stage I crack and estimated ΔK_{Imax} value. In this estimation the temperature dependence of ΔK_{Imax} value was neglected, and ΔK_{Imax} value fitted for all data. The dependence of the initiation site size on the maximum stress range could be accounted for by an assumption that the microcrack growth is controlled by the critical condition, ΔK_{th} =constant. Thus the detection of subsurface fatigue crack initiation in wider stress range at lower temperature strongly depends on the microcrack growth in Stage I. The modeling that was based on the linear fracture mechanics under the Mode I condition also provided a good estimate of the stress intensity range of fatigue crack growth, enabling the estimation of the crack propagation life.[10] The calculated crack propagation life was less than a tenth of the number of cycles to failure over 10^6. These are useful to promote a better understanding of subsurface fatigue crack initiation and propagation.

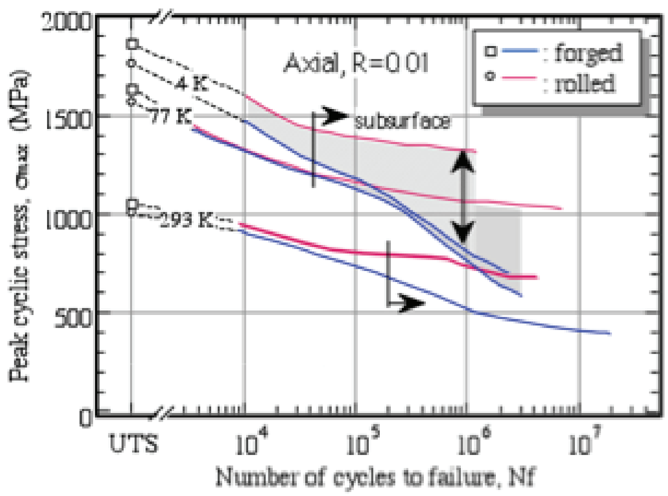

FIGURE 1. S-N curves of a Ti-6Al-4V alloy with two kinds of conditions in microstructure at low temperatures.[2]

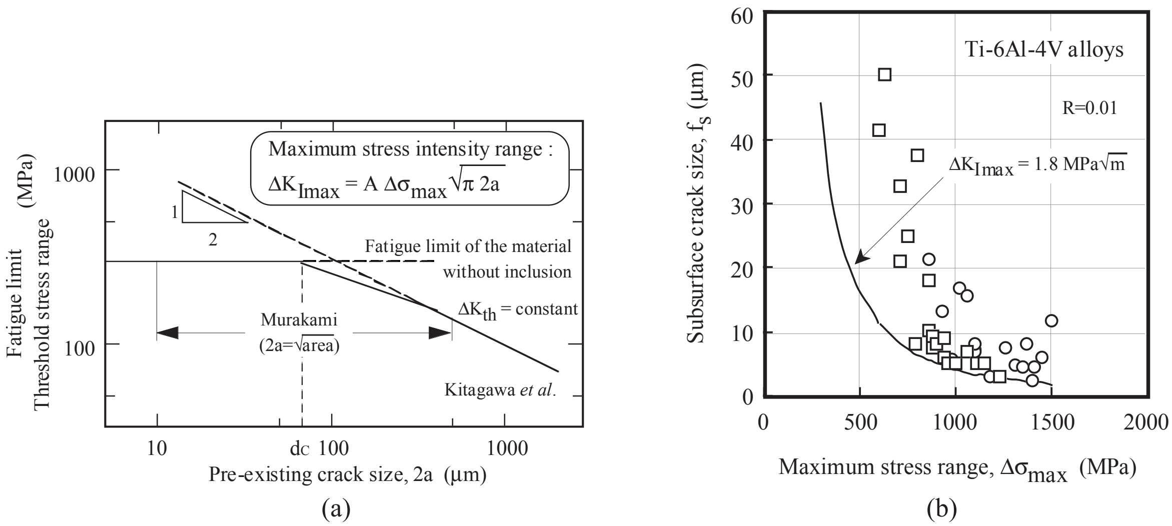

FIGURE 2. Dependence of threshold conditions for fatigue crack growth of a microcrack on stress range (a) and size of the subsurface crack initiation sites in Ti-6Al-4V alloy (b).[1]

Origin of Subsurface Crack Initiation Site

The microcrack growth and/or coalescence model can excellently explain the formation process of Stage I crack with a critical size. This involves the process of microcrack growth during a large number of fatigue cycles, not instantaneously [11-14]. A new explanation of microcrack growth proposal [11] may further the understanding of the damage stage. Although the morphology and size of subsurface crack initiation sites are affected by stress level and subsurface crack origins such as transgranular crack, intergranular crack, non-metallic particles and segregation, the microcrack growth concept normally gives a good solution.

The mechanism of subsurface crack generation, however, has not been clarified yet, especially in the local damage and microcracking stages. Figure 3 summarizes fatigue crack initiation mechanisms giving an integrated model for both surface crack initiation and subsurface initiation sites. The dislocation structures in high-cycle fatigue are fairly planar for both austenitic steel [12] and titanium alloys [14]. The very localized deformation processes have been found to be decisive for subsurface fatigue crack generation at lower stress levels such as the elastic incompatibility at boundaries, where only a very small fraction of plastically deformed grains was detected. Heterogeneous microplasticity due to planar slip and restricted system is considered to play an important role on making the subsurface crack.

To reduce localized strain incompatibility at grain boundaries, fine-grained duplex microstructure was obtained through partial recrystallization. The treated material showed considerably improved high-cycle fatigue strength and more homogenous plastic deformation as illustrated in Figure 4 [15-16]. Both the grain refinement and the work hardening due to the increase of the average dislocation density may commonly play an important role in the fatigue behavior of severely deformed materials. To gain a better understanding of the cyclic behavior of fine-grain-structure materials, the effects of (1) randomly distributed crystal orientation, (2) fine second-phase dispersion, and (3) lowering the local yield stress of pseudo-elastic grains on high resistance to microcrack growth should be considered, since the distribution of microcracks is closely related to the grain structure and/or second-phase structure.

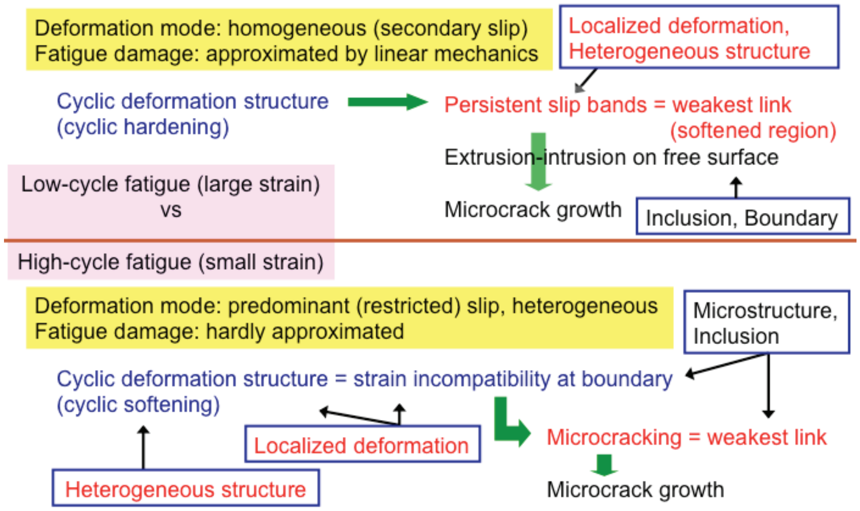

FIGURE 3. Schematic illustration of fatigue crack initiation mechanism as an integrated model.

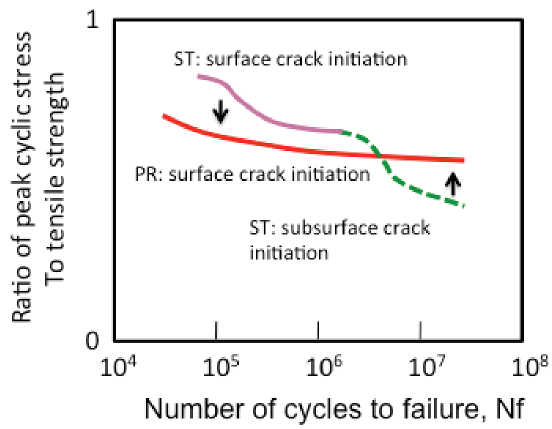

FIGURE 4. Schematic S-N curves showing modification by partial recrystallization.[15]

THERMAL ACTIVATION PROCESS

Strain Rate Dependence of Stress-Strain Curves

As a description of stress-strain curves of Ti alloys, Moriya *et al*.[4] have proposed the following equation:

$$\sigma = a\left(b+\varepsilon_p\right)^N + K\dot{\varepsilon}^m \tag{1}$$

where a, b, N. K and m are material constants, σ true stress, ε_p true plastic strain and $\dot{\varepsilon}$ strain rate. The first term of Eq. (1) was called the “base curve”, which was obtained experimentally by a series of stress-relaxation measurements during tensile deformation. The test consists of periodically holding the crosshead at constant displacement measuring the decrease of applied stress with time as shown in Figure 5. After sufficient stress-relaxation cycles, the changes in load and displacement become very small and difficult to be detected. Such stabilized stress and strain provide a point on the flow curve, and those points obtained by repeated crosshead-arresting tests at various strains construct the base curve. The base curve was well fitted with Swift's equation. To determine the base curve, test temperature is an important parameter; larger load-drops as well as higher flow stress occur at cryogenic temperature.

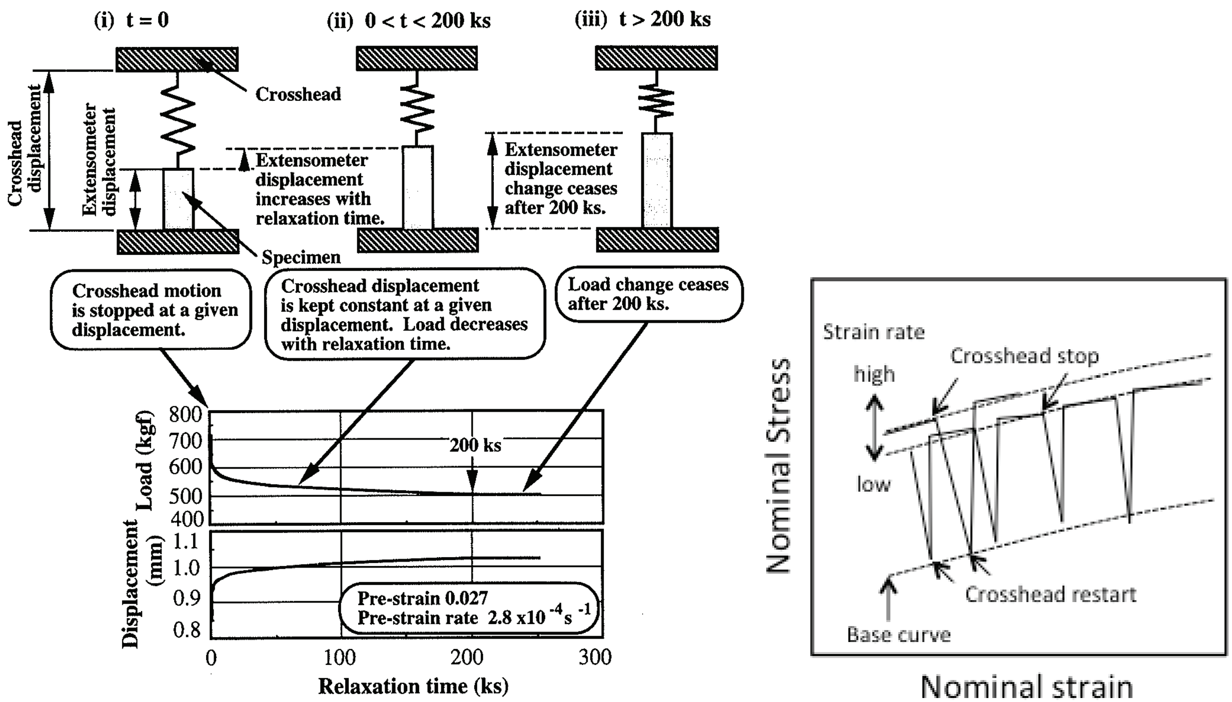

FIGURE 5. Schematic illustration of the crosshead-arresting test.[4]

Description of Stress-Strain Curves Based on Thermal Activation Model

Kocks [17] has proposed an empirical work-hardening law that relates the work-hardening rate to the stress, based on thermal activation processes for dislocation density evolution. This work-hardening law has been developed to describe stress-strain curves by Mecking and Kocks [18] and Follansbee and Kocks [19], i.e., the so-called Kocks–Mecking (KM) model. Tsuchida et al.[5-7] adopted the KM model to clarify the effects of temperature and strain rate on flow stress. Crosshead-arresting tests were conducted and found to provide flow curves at the strain rate of 10^{-9} s^{-1} that were apparently dependent on test temperature. This strain rate correlates with the strain rate of the engineering limit of strain detection. The athermal stress was much lower than the flow curve at 10^{-9} s^{-1} and was difficult to estimate from the stress relaxation behavior below room temperature.

STRAIN INCOMPATIBILITY ANAYSIS BASED ON FULL CONSTRAINTS MODEL

Restriction of Slip Systems at Lower Temperature

The restriction of other slip systems results from their CRSSs. Moreover, both plastic and elastic deformations coexist in polycrystalline specimens, since the relative deformation depends on crystal orientation. The plastic deformation on the facet plane hardly yields and the elastic field normal to the facet plane has to increase. The plastic deformation, that relaxes the stress field under the tension or simple shear mode in α-titanium alloy at low temperatures, was evaluated using the Taylor model [2]. The model was employed because experimental analyses can hardly demonstrate cracking behavior itself. In areas of the largest amount of plastic work the α grains, around tensile stress axis of <0001>, were hardly relaxed, since the <c+a> pyramidal slip systems and twinning were inactive. Thus, the accumulated tensile stress along <0001> may be responsible to initial microcracking on {0001} and for crack opening [20]. The localized basal slip on {0001} under the simple shear mode may assist the growth of microcracks. The simple shear mode on (01-10) also led to induced localized slip of {10-10}<1-210> or {0001}<1-210>. The growth rate of microcracks on {01-10} was higher than that on {0001}.

Evaluation of Grain Interaction Induced by Planar Slips

Although it has been commonly noted that a local stress concentration due to the grain interaction (incompatibility) at the grain boundaries results in transgranular cracking or intergranular cracking to reduce the stress, the cracking mechanisms have yet to be clarified. An accommodation deformation model to relax incompatibility between soft (yielded) and hard (non-yielded) grains was proposed for austenitic steel [21]. Dislocation arrays were installed in the soft grain to investigate the effect of secondary slip on accommodating the displacement incompatibility due to adjacent grain interactions at the grain boundary. To accommodate the displacement incompatibility at the grain boundary, slip systems in the adjacent grains were required in almost all orientations. Around the orientation at which the secondary plastic deformation was the hardest to achieve, three slip systems were operated on different octahedral slip planes in areas of strain accumulation with high displacement incompatibility. However, the displacement incompatibility was not fully accommodated, and a stress field remains near the normal to {111}. The combination of sufficient stress concentration to open the grain boundary and the assembly of dislocations on the three slip systems at the grain boundary may be the cause of intergranular cracking. This conclusion agrees well with the experimental evidence of intergranular cracking in nitrogen-strengthened austenitic steel, where mismatched line traces on the matching facets of opposing fracture surfaces were observed [12].

SUMMARY

The advantage of cryogenic mechanical tests has been described to promote better understanding of deformation and microstructural cracking in high-strength alloys. Subsurface cracks are very common Stage I initiation sites in high-cycle fatigue at low temperatures for high strength alloys. Heterogeneous micro-plasticity due to planar slip and restricted slip systems is considered playing an important role in the creation of subsurface cracks. The crack initiation site size is mainly controlled by ΔK_{th} the stress intensity threshold. Thus, cryogenic fatigue tests can provide a big advantage to analyze subsurface crack generation clearly. The flow stress curve analysis at low temperatures also provides a clearer description of alloy deformation.

ACKNOWLEDGMENTS

We thank T. Ogata, T. Yuri, H. Moriya, N. Tsuchida, S. Morooka and M. Morita for their help.

REFERENCES

1. O. Umezawa and K. Nagai, *ISIJ International*, **37**, 1170-1179 (1997).
2. O. Umezawa, T. Ogata, T. Yuri, K. Nagai and K. Ishikawa, in *Advances in Cryogenic Engineering Materials*, edited by R.P. Reed, Vol. 40, Plenum Press, NY, 1994, pp. 1231-1238.
3. O. Umezawa, M. Morita, T. Yuasa, S. Morooka, Y. Ono, T. Yuri and T. Ogata, ICMC2013, to be submitted.
4. H. Moriya, K. Nagai, Y. Kawabe and A. Okada, *ISIJ International*, **37**, 1016-1022 (1997).
5. N. Tsuchida, H. Moriya, Y. Tomota, O. Umezawa and K. Nagai, *ISIJ International*, **40**, 84-90 (2000).
6. N. Tsuchida, Y. Tomota, H. Moriya, O. Umezawa and K. Nagai, *Acta Materialia*, **49**, 3029-3038, (2001).
7. N. Tsuchida, E. Baba, O. Umezawa, K. Nagai and Y. Tomota, *ISIJ International*, **44**, 209-213 (2004).
8. H. Kitagawa, S. Takahashi, C. M. Suh and S. Miyashita, in *Fatigue Mechanisms*, ASTM STP 675, Philadelphia, 1978, pp. 420-447.
9. Y. Murakami, *Tetsu-to-Hagane*, **75**, 1267-1277 (1989).
10. M. Hamada and O. Umezawa, *ISIJ International*, **49**, 124-131 (2009).
11. O. Umezawa, K. Nagai and K. Ishikawa, *Tetsu-to-Hagane*, **75**, 159-166 (1989).
12. O. Umezawa and K. Nagai, *Metall. Mater. Trans. A*, **29A**, 3017-3028 (1998).
13. O. Umezawa and K. Nagai, *Metall. Mater. Trans. A*, **29A**, 809-822 (1998).
14. H. Yokoyama, O. Umezawa, K. Nagai, T. Suzuki and K. Kokubo, *Metall. Mater. Trans. A*, **31A**, 2793-2805 (2000).
15. O. Umezawa, *Metall. Mater. Trans. A*, **35A**, 543-553 (2004).
16. O. Umezawa, *ISIJ International*, **49**, 1624-1629 (2009).
17. U.F. Kocks, *J. Eng. Mater. Tech.*, **98**, 76-85 (1976).
18. H. Mecking and U.F. Kocks, *Acta metal.*, **29**, 1865-1875 (1981).
19. P.S. Follansbee and U.F. Kocks, *Acta metal.*, **36**, 81-93 (1988).
20. M. Morita and O. Umezawa, *Materials Transactions*, **52**, 1595-1602 (2011).
21. M. Morita and O. Umezawa, *ISIJ International*, **52**, 1163-1171 (2012).